Journal of Nepal Geological Society, 2024, Vol. 67, pp. 127–138
https://doi.org/10.3126/jngs.v67i1.74591

Spatial analysis of causative factors for landslide susceptibility mapping in parts of Makwanpur District, central Nepal

Champak Babu Silwal, *Ashok Sigdel, Pratima Subedi, Subash Acharya and Deepak Chamlagain

Department of Geology, Tri-Chandra Multiple Campus, Tribhuvan University, Kathmandu Nepal
**Corresponding author's email: ashok.sigdel@trc.tu.edu.np*

ABSTRACT

Landslides pose a persistent and severe risk, frequently resulting in substantial harm to both people and infrastructures in Nepal. Understanding the underlying cause-and-effect dynamics of these events is crucial for effective mitigation measures to minimize their impacts. This research delves into assessing the susceptibility to landslides in the Thaha, Bhimphedi, Kailash, and Indrasarobar Rural Municipalities of the Makawanpur district. Considering the area's predisposition to landslides and soil erosion, exacerbated by the highly dissected topography and monsoon rainfall, this region is critically important for landslide susceptibility mapping. Using the satellite and aerial images, an inventory of 230 landslides was prepared. A total of nine landslide influencing factors including slope, aspect, curvature, distance to road, distance to stream, landuse/landcover, topographic position index, lithology, and lineament density were integrated to produce the landslide susceptibility index using the Analytic Hierarchy Process (AHP). Landslide susceptibility map thus generated was divided into five classes ranging from very low to very high susceptible zones. Validation of the susceptibility map was done using the landslide inventory, where the area under the Receiver Operating Characteristic (ROC) curve indicated a success rate of 0.727, demonstrating a commendable accuracy in predicting landslide occurrences. Similarly, the landslide density along with different susceptibility classes also indicate better performance to predict the susceptible zone. This susceptibility map can be very useful for planning the effective landslide disaster response and mitigation in the study area.

Keywords: Landslide Susceptibility; Analytical Hierarchy Process (AHP); Geographical Information System (GIS); Makawanpur; Central Nepal

Received: 16 May 2024 **Accepted:** 6 November 2024

INTRODUCTION

Landslides are one of the most abundant and common natural hazards that cause significant damages in a mountainous country like Nepal (Bhandary et al., 2006). Nepal Himalaya, characterized by the rugged terrain, harbors a complex interplay of geological, climatic, and anthropogenic factors render it as the region with high susceptiblity to landslides (Dahal and Dahal, 2017). Landslide not only pose significant threats to human life and infrastructure but also impede socioeconomic development in this region of immense cultural and ecological significance.

Landslides in the Nepal Himalaya have been increasing in recent years due to a complex interaction of the factors, including rapid urbanization, deforestation, erratic precipitation patterns attributed to climate change, and the geological fragility inherent to mountainous terrains (McAdoo et al., 2018; Vaidya et al., 2019; Muñoz-Torrero Manchado et al., 2021). The devastating earthquakes of 2015 further exacerbated this vulnerability, underscoring the urgent need for proactive measures to mitigate landslide risks and enhance resilience (Roback et al., 2018).

Landslide susceptibility mapping is a crucial aspect that identifies landslide-prone areas based on various causative factors such as topographical, geological, hydrological, and environmental parameters and the history of landslide occurrences (Glade and Crozier, 2005; Pourghasemi et al., 2013). Effective landslide susceptibility mapping plays a pivotal role in understanding the spatial distribution and underlying causes of landslide occurrence, thereby facilitating informed decision-making for land use planning, disaster preparedness, and infrastructure development. Previous studies have demonstrated the efficacy of susceptibility mapping of landslide-prone areas and identifying the primary drivers governing susceptibility patterns in mountainous terrains like Nepal Himalaya (Kayastha et al., 2012; Regmi et al., 2016; Acharya et al., 2017; Thapa et al., 2022).

Recent studies have introduced various methodologies for assessing landslide susceptibility, including qualitative, quantitative, and semi-quantitative approaches (Das et al., 2023). Among these, the Analytic Hierarchy Process (AHP) has emerged as a preferred method due to its ability to simplify complex decision-making by quantifying subjective judgments and synthesizing them into a structured model (Saaty, 1980). Unlike purely qualitative methods, which rely on expert opinion and historical data, AHP provides a more reliable and transparent decision-making process. It is particularly advantageous over machine learning and deep learning algorithms, which require extensive data and computational resources, making AHP more accessible in regions with limited data availability (Neaupane and Piantanakulchai, 2006; Ayalew et al., 2005; Akgun et al., 2010). This balance of structured analysis and practical application has established AHP as a valuable tool for both local and regional-scale landslide susceptibility assessments.

Makawanpur district in Central Nepal is a critical area for examining landslide susceptibility due to its challenging terrain and environmental conditions, which heighten the risk of natural disasters. The region, particularly around Kulekhani, is significantly threatened by both landslides and soil erosion (Sthapit, 1996; Pradhan et al., 2012; Shrestha et al., 2024). The rugged topography, characterized by steep slopes, coupled with the region's monsoon rainfall patterns, creates a condition that heightens the susceptibility to landslides. The natural susceptibility to slope failures and soil erosion within the region is intensified by the complex interplay among the morphological, geological, and anthropogenic activities, heightening the risk of damage to existing infrastructure.

To date, there has been a notable absence of studies focusing on landslide mapping and susceptibility zonation in the study area. Hence, the current research is centered on conducting landslide susceptibility mapping utilizing the Analytic Hierarchy Process (AHP) method in conjunction with Geographic Information Systems (GIS). This approach aims to delineate the susceptibility zone of the area, thereby assisting in the mitigation and management of potential hazards associated with future landslide occurrences. The mapping process takes into account various factors including topographical, geological, and anthropogenic features to provide a comprehensive understanding of landslide susceptibility in the region.

STUDY AREA

Makawanpur district, situated in Bagmati Province, central Nepal, spans an area of 2,426 km$^{2.}$ The district is situated between latitudes 27˚ 21' to 27˚ 40' N and longitudes 84˚ 41' to 84˚ 35' E. The study area is located in the northern part of Makawanpur district (Fig. 1), encompassing four Rural Municipalities: Thaha, Indrasarowar, Kailash, and Bhimphedi, with an area of about 739 km^2. The district boasts diverse topography, with elevations ranging from 337 to 2535 meters above mean sea level (Fig. 1). The major stretch of the Kanti Lokpath and the Tribhuvan Rajpath passes the study area making it strategic alternative connection between the East-West Highways and the Kathmandu, the federal capital of Nepal. Geologically, it is divided into three tectonic divisions: the Siwalik Group, the Nawakot Complex and the Kathmandu Complex of the Lesser Himalaya (Stöcklin and Bhattarai, 1980). The study area mostly covers the Bhimphedi Group and Phulchauki Group of the Kathmandu Complex.

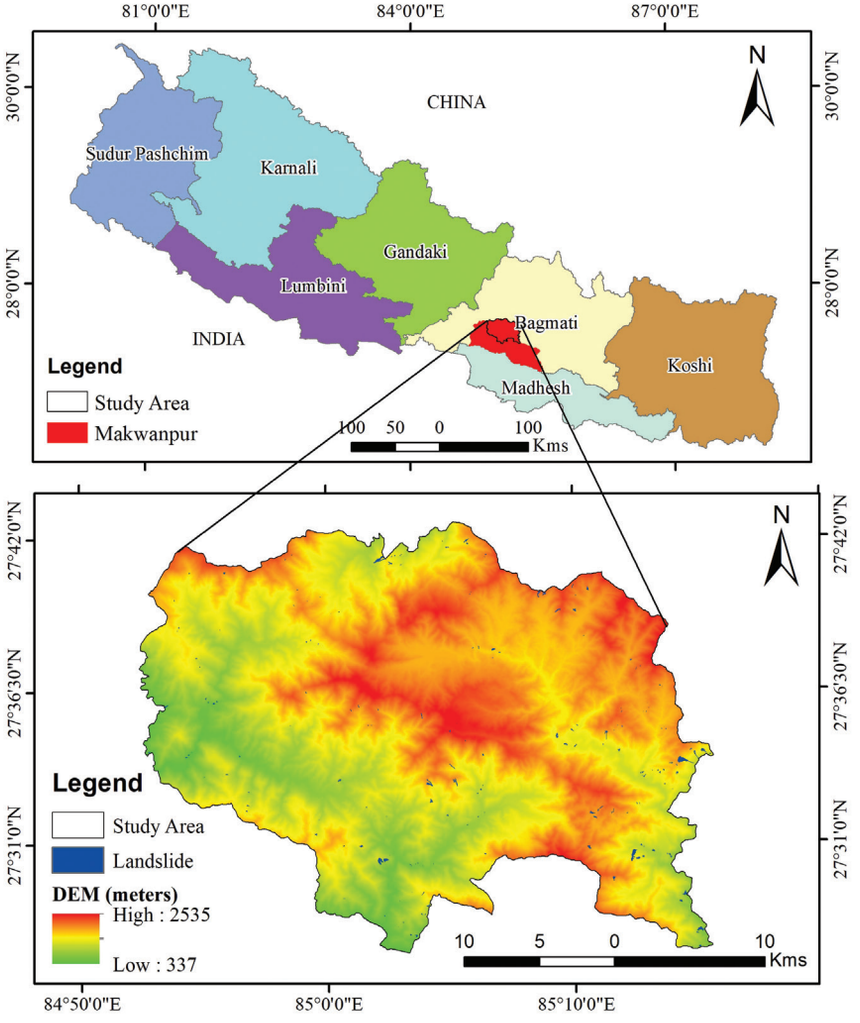

Fig. 1: Location map of the study area along with the elevation and the landslide distribution.

METHODOLOGY

Assessment of a landslide susceptibility involves crucial steps (Fig. 2), with data collection being vital. In this study, nine factors were determined to be significant contributors for landslide events. The factors were selected based on the characteristics of study area and the observed landslides, expert knowledge, and data availability. Also the factors identified are well adopted and most frequently used for landslide susceptibility analysis in the Himalaya (Das et al., 2023). These includes slope, aspect, curvature, distance to road, distance to stream, land cover/land use, Topographic Positioning Index (TPI), lithology, and lineament density. Various data sources were accessed, including Google Earth and satellite images (ALOS-PALSAR, 12.5m terrain data), Landuse/Landcover map (ESA, Sentinel 2A, 10m), Open Street map, Geological map (Stöcklin and Bhattarai, (1980), and 1:25000 scale topographic maps from the Department of Survey, Government of Nepal.

Weight and rank calculations were performed using the AHP by Saaty (1980). These factors and their respective classes were then integrated through the weighted Linear Combination (WLC) approach to generate the Landslide Susceptibility Index (LSI). The prepared LSI map was then validated using the landslide inventory of the area using the area under the Receiver Operating Characteristics (ROC) curve. The validated LSI map was then classified into different levels of landslide susceptibility zones.

Landslide inventory map

Landslide inventory mapping is a detailed representation of historical landslides in a specific area, achieved through analyzing aerial and satellite imagery, studying existing literature, and conducting extensive field investigations. Such mapping is crucial for understanding landslide susceptibility and exploring the factors that predispose these events. In this study a reliable landslide inventory map was prepared by the visual interpretation of the satellite and aerial images and conducting on-site visits as a validation. The inventory is compiled during the desk study and later validated by field observations along the road section of the Tribhuvan Highway, the Kanti Lokpath and the Kulekhani - Chitlang road section. The landslides were identified observing the active and old landslide scarps, detailed fieldwork, historical landslide record, and time series satellite and aerial imagery analysis. The landslides were digitized into polygons, showing the spatial distribution using GIS environment.

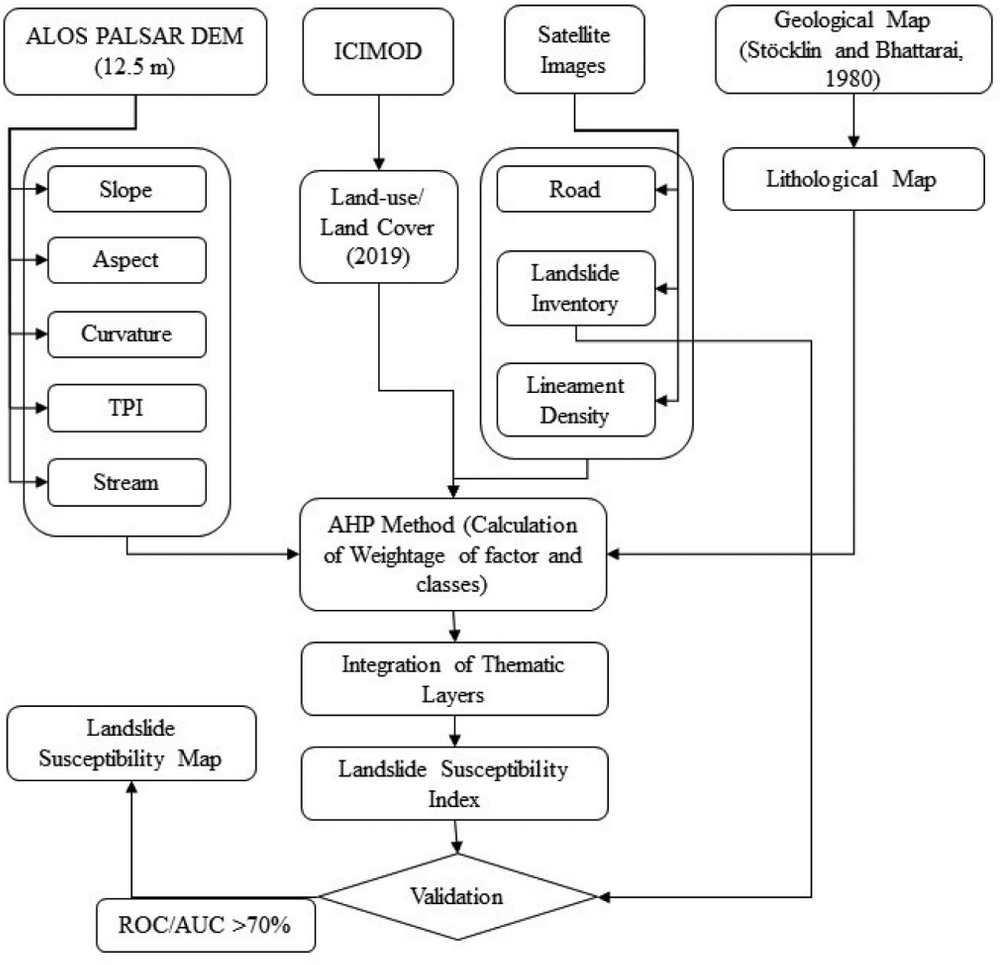

Fig. 2: Flowchart showing the detailed procedure of the landslide susceptibility analysis.

Thematic factors

To delineate the landslide susceptibility zones in the study area, a total of nine key parameters were selected for this study (Fig. 2). The ALOS PALSAR 12.5 m high resolution terrain data from the repositories of Alaska Satellite Facility (ASF) – Distributed Active Archive Center (DAAC) has been used as Digital Elevation Model (DEM), which forms the base to produce the slope, aspect, curvature, and distance to stream in the GIS environment. The thematic layers were prepared and analyzed with 12.5*12.5 m resolution to match the raster cell size of the available DEM.

Slope

The inclination of the land, known as slope, is widely recognized as a significant factor contributing to landslides and has been dominantly used in the susceptibility analysis. Majority of the studies related to the landslide susceptibility analysis emphasizes that steeper slopes correlate with increased landslide risk, underscoring the importance of slope angle in assessing landslide susceptibility (Das et al., 2023). In the presented study, a slope map derived from DEM is categorized into five classes: 0-15°, 15°-25°, 25°-35°, 35°-45°, and >45° (Fig. 3a).

Lithology

Lithological units indicate a wide range of landslide sensitivity values and are crucial for identification of susceptible zones as the landslide events are dependent on the intrinsic geo-mechanical properties and associated deformation structures (Hong et al., 2016). Based on the lithological composition of the different formations from the geological map of Stöcklin and Bhattarai (1980), the lithological map of the study area has been extracted. Altogether, there are seventeen formations in the study area namely the Benighat Slate and Robang Phyllite of the Upper Nawakot Group, Raduwa Formation, Bhainsedhoban Marble, Kalitar Formation, Chisapani Quartzite, Kulikhani Formation, and Markhu Formation of the Bhimphedi Group, Tistung Formation, Sopyang Formation, Chandragiri Limestone, and Chitlang Formation of the Phulchauki Group, along with the intrusive granitic rocks, rocks of Siwalik and the quaternary deposit. These formations are further combined according to their common lithology to create the lithological map of the study area. The lithology is divided into nine classes: basic rock, quartzite, granite basic and gneiss, dolomite, marble, phyllite, schist, rocks of Siwalik, and quaternary sediments (Fig. 3b).

Land use/Land cover

Modifications in land use and land cover due to deforestation, unregulated road building, and associated human influences can destabilize slopes, potentially contributing to increased occurrences of landslides. This factor has been identified as the major factor used for landslide susceptibility mapping in the Himalayan region (Das et al., 2023). In the current analysis, the landuse and land cover map was extracted from the repositories of European Space Agency (ESA), Sentinel 2A with the resolution of 10m and was reclassified into five classes: River/Waterbody, Trees (Forest), Grassland, Cultivation, and Built area (settlements) (Fig. 3c).

Lineament density

Lineaments provide insights into the structural makeup of the underlying rock formations. Typically, they are identified as vulnerable surface features such as joints, faults, and shear zones. These attributes elevate the risk of landslides occurring (Pathak, 2016). The lineament map was prepared using the image interpretation of Google Earth, that allows the observation of the earth's surface using perpendicular and oblique viewing perspective. This method of identifying lineaments is highly reliable and has been adopted widely (Lawal et al., 2022). The lineament density map was prepared and classified into three classes (low, moderate and high) based on the spatial density of lineaments in the area (Fig. 3d) using line density tool in GIS.

Distance to Stream

To analyze the impact of stream proximity on landslide occurrence, a stream network map was generated from the DEM in GIS environment. The buffer zones of different distances from the stream were created using the Euclidean distance method (Pradhan and Kim, 2020; Huang et al., 2022) and were categorized as 0-50 m, 50-150 m, 150-300 m, 300-450 m, and >450 m (Fig. 4a).

Distance to Road

The proximity to roads is often considered a significant anthropogenic factor contributing to landslide susceptibility (Pourghasemi et al., 2012). The road network in the study area was extracted from the Open Street Map (OSM) available in Google Earth. The road network was used to produce the buffer of different distance using the Euclidean distance method in GIS environment and was segmented into five classes: 0-100 m, 100-200 m, 200-300, 300-400 m, and >400 m (Fig. 4b).

Topographical Position Index (TPI)

The TPI measures the elevation difference between a cell (DEM) and the mean elevation of its surrounding with the window size of 33 * 33 cells (Seif, 2014). A TPI close to zero signifies flat or mid-slope terrain, whereas higher TPI values suggest ridges and steep slopes more susceptible to landslides (Roy et al., 2023). The TPI map was classified into three classes river valley (<-10), slope land (-10 - 25), and Hilltop/Spur (>25) (Fig. 4c).

Curvature

Plan curvature refers to the curvature of topographic contours. It influences how landslide material and water converge or diverge in the direction of landslide movement (Carson and Kirkby, 1972). In the present study, curvature of the slope was generated using the DEM in GIS environment. The curvature map was then categorized as concave, flat, and convex (Fig. 4d).

Aspect

Aspect is a key parameter utilized in assessing landslide susceptibility due to its influence on various factors such as weathering, vegetation, soil moisture, and hillslope (Garcia-Rodriguez et al., 2008). Additionally, meteorological elements like rainfall and sunlight exposure manifested by the slope aspect, play a significant role in landslide occurrence (Komac,

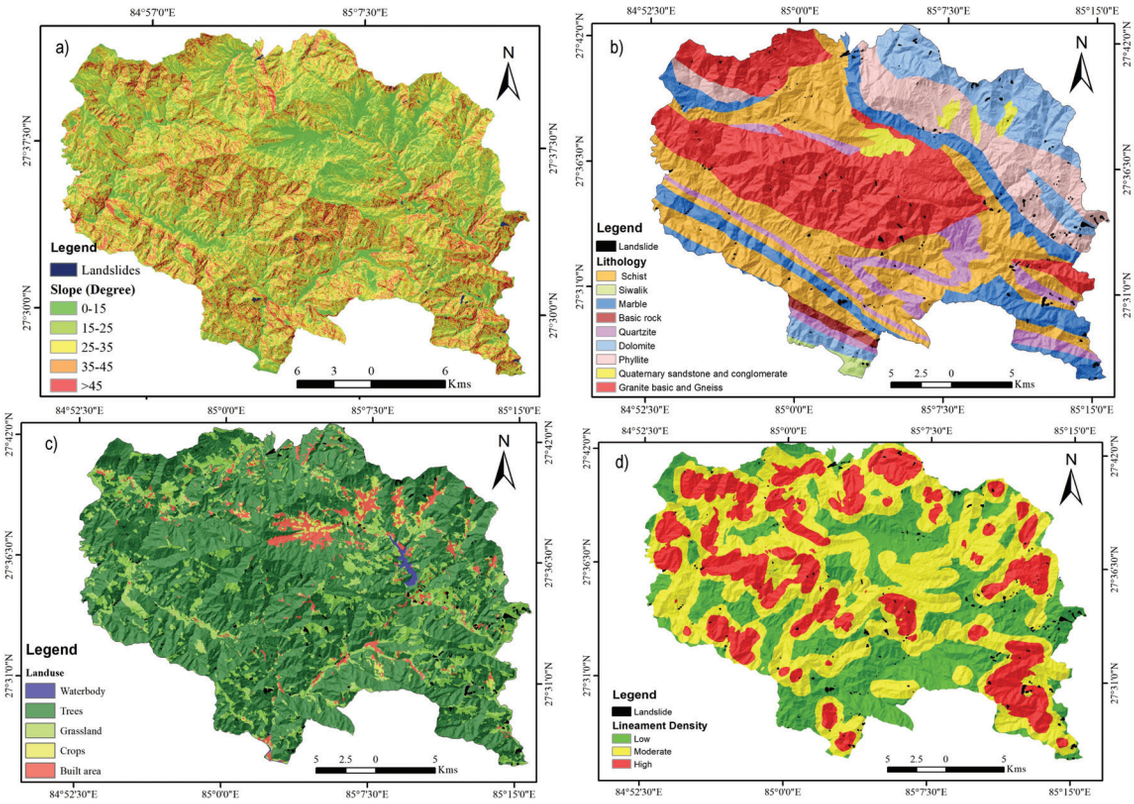

Fig. 3: Thematic layers used for landslide susceptibility zonation, a) Slope in degree, b) Lithology (after Stöcklin and Bhattarai, 1980), c) Landuse map (ESA, sentinel 2A), d) Lineament Density map

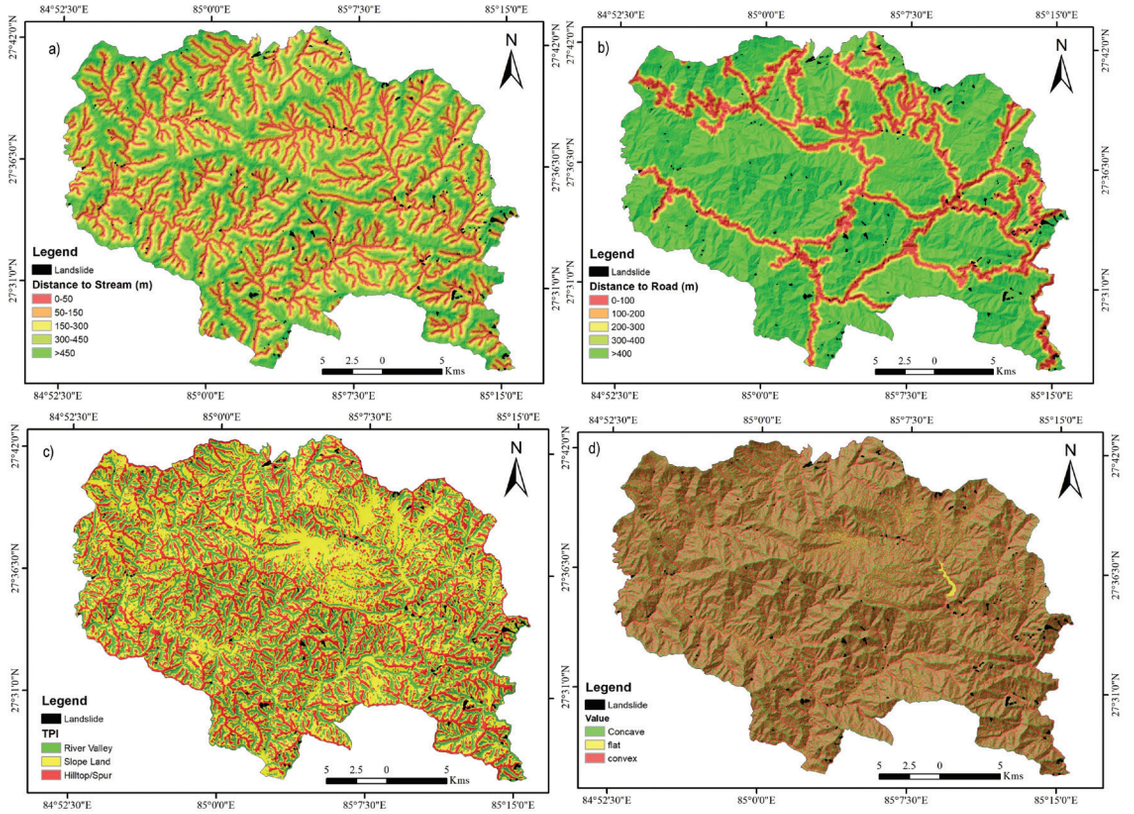

Fig. 4: Thematic layers used for landslide susceptibility zonation, a) Distance to stream, b) Distance to road, c) Topographic Position index (TPI) d) Curvature of the slope.

2006).

The Aspect map was generated using the DEM in spatial analysis in GIS environment, which is further classified into nine different classes as Flat (-1), North (0° - 22.5° and 337.5° - 360°), Northeast (22.5° - 67.5°), East (67.5° - 112.5°), Southeast (112.5° - 157.5°), South (157.5° - 202.5°), Southwest (202.5° - 247.5°), West (247.5° - 292.5°), and Northwest (292.5° - 337.5°), following the direction of slope facets (Fig. 5).

Weight and rank calculation

AHP method is one of the most significant semi-quantitative methods for landslide susceptibility assessment and prediction (KC et al., 2024). This method was first propounded by Saaty (1977) in social science studies and later used in different scientific studies that uses Multi-Criteria Decision Analysis (MCDA). The method used the pairwise comparison matrix of N*N order where N is the number of factors under consideration. The comparison is performed using a relative importance scale ranging from 1 to 9 (Saaty, 1980). A value of 1 indicates equal importance whereas 9 denotes extreme importance. The pairwise comparison matrix is normalized to calculate the weight for each factor.

The AHP offers a valuable feature in assessing pair-wise rating inconsistency making it more robust and reliable. Eigenvalues (λ) help quantify a consistency measure that indicates inconsistencies in pair-wise ratings. Saaty (2000) noted that in a consistent reciprocal matrix, the largest eigenvalue (λmax) equals the number of comparisons (N).

In addition, the Consistency Ratio (CR) serves as an index of consistency, indicating the likelihood that the judgment matrix was randomly generated (Saaty, 1977). The CR is calculated using the Consistency Index (CI), derived from the largest eigenvalue (λmax) and the number of factors under consideration (N) and Random Consistency Index (RI) (Saaty, 2000). Saaty (1977) indicated that CR value equal to or smaller than 10% signifies acceptable inconsistency.

Table 1 presents the pairwise comparison matrix for landslide susceptibility, encompassing the nine thematic layers. The significance of these factors and their classes was evaluated based on the authors' expertise and knowledge acquired from previous assessments of landslides in similar terrain

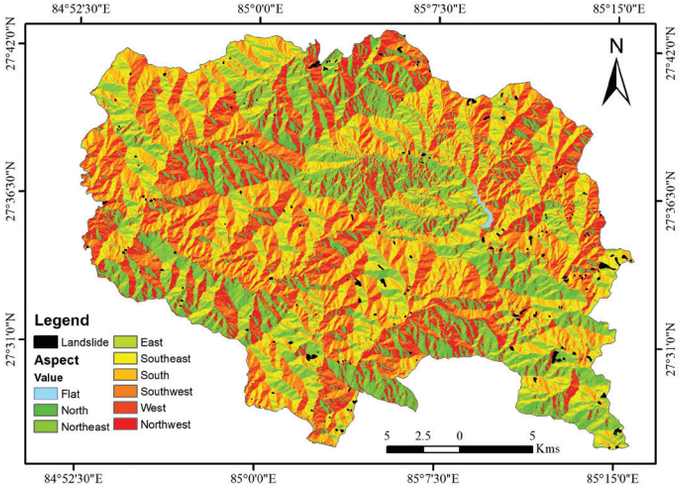

Fig. 5: Thematic factor as Aspect of slope facet within the area.

Table 1: Pairwise comparison matrix used for the calculation of normalized comparison matrix to calculate the weightage of factors.

	Slope	Geology	LD	Landuse	Stream	Road	TPI	Aspect	Curvature
Slope	1	2	2	2	3	3	3	4	4
Geology	1/2	1	2	2	2	3	3	3	4
LD	1/2	1/2	1	2	2	2	3	3	3
Landuse	1/2	1/2	1/2	1	2	2	2	3	3
Stream	1/3	1/2	1/2	1/2	1	2	2	3	3
Road	1/3	1/3	1/2	1/2	1/2	1	2	2	2
TPI	1/3	1/3	1/3	1/2	1/2	1/2	1	2	1
Aspect	1/4	1/3	1/3	1/3	1/3	1/2	1/2	1	1
Curvature	1/4	1/4	1/3	1/3	1/3	1/2	1	1	1

*LD=Lineament density, TPI= Topographic Position Index

and geological conditions (Pradhan et al., 2012; Acharya and Pathak, 2017; Regmi et al., 2014). The CR value (0.37) and average λmax (9.288) for the factors lies within the acceptable limits (Saaty, 1980). Through a comprehensive statistical analysis of the AHP method, weightage percentages, average λmax values, and CR values for each factors and their respective classes were derived as detailed in Table 2.

Table 2: Weightage of the factors and their respective classes calculated using AHP method along with maximum Eigenvalue (λmax), Consistency Ratio (CR) and Random Consistency Index (RI).

Factors	Weight%	Classes	Weight %	
Slope	23.33	0-15˚	15	λmax = 5.188, CR = 4.2%, RI=1.12
		15˚-25˚	7	
		25˚-35˚	15	
		35˚-45˚	30	
		>45˚	44	
Lithology	18.55	Schist	10	λ_{max} = 9.626, CR= 5.4%, RI=1.45
		Siwalik	25	
		Marble	16	
		Basic Rock	3	
		Quartzite	8	
		Dolomite	19	
		Phyllite	13	
		Quaternary sediment	2	
		Granite and Gneiss	4	
Land use	12.02	Built area	12	λmax = 5.194, CR= 4.3%, RI=1.12
		Waterbody	7	
		Cultivation	17	
		Grassland	26	
		Forest	39	
Lineament Density	14.71	Low	16	λmax = 3.009, CR= 1%, RI=0.58
		Moderate	29	
		High	53	
Distance to Stream	9.89	0-50m	32	λmax = 5.195, CR= 4.3%, RI=1.12
		50m-150m	24	
		150m-300m	19	
		300m-450m	14	
		>450m	11	
Distance to Road	7.32	0-100m	36	λmax = 5.114, CR= 2.5%, RI=1.12
		100m-200m	25	
		200m-300m	18	
		300m-400m	12	
		>400m	9	
Topographical Position Index	5.59	River Valley	44	λmax = 3.018, CR= 1.9%, RI=0.58
		Hill Slope	38	
		Hilltop/ Spur	16	
Curvature	4.36	Concave	45	λmax= 3, CR= 0%, RI=0.58
		Flat	9	
		Convex	45	
Aspect	4.23	Flat	3	λmax= 9.361, CR= 3.1%, RI=1.45
		North	4	
		Northeast	6	
		East	16	
		Southeast	28	
		South	19	
		Southwest	13	
		West	8	
		Northwest	3	

Landslide susceptibility mapping and validation

The Landslide Susceptibility Index (LSI) in the AHP was calculated using a weighted linear combination model for each pixel. This involved summing the product of each factor's weight (Wi) and its corresponding class weight (Ri) for the referenced landslide-triggering factors, as represented in the following equation:

$$LSI = \sum_{i=1}^{n} (Wi \times Ri)$$

Here, "n" represents the number of factors considered in the analysis. The equation captures the weighted contribution of each factor to the overall landslide susceptibility index for a given pixel within the study area.

Validation of predictive models is crucial for creating meaningful landslide susceptibility maps and various validation techniques exist for this purpose. The ROC curve gives the area under the curve (AUC) and it is a measure of goodness of fit used to assess the performance of a model, particularly in the context of predicting events like landslides. The AUC value indicates the model's effectiveness in predicting both the presence and absence of landslides. The AUC value ranges from 0 to 1, with a higher value indicating a better performance of the model (Yasilnacar and Topal, 2005). The AUC greater than 70% is generally accepted as good prediction of the model (Silwal et al., 2023). The generated LSI map was overlain with landslide inventory map to calculate the True Positive Rate (Sensitivity) and False Positive Rate (1- Specificity) used to prepare the ROC curve. The validated LSI map was then classified as very low, low, moderate, high and very high susceptibility zones.

RESULT

Landslide inventory

The landslide inventory displays the spatial distribution of landslide data (Fig. 6). Altogether 230 large and small scales landslides ranging from 22 – 159090 m^2 were identified and located (Fig. 6). The landslides cover a total area of about 1.62 km^2, which is 0.22% of the total study area. This inventory map is later used for the validation of Landslide Susceptibility model.

Landslide susceptibility analysis

The susceptibility map was categorized into five classes namely very low, low, moderate, high and very high susceptible zones (Fig. 7). The percentage distribution of areas of very low susceptible zone is 18.58%, followed by 28.95% in low susceptible, 26.38% in moderate susceptible, 18.25% in high susceptible, and 7.84 % in very high susceptible zones.

Validation of the susceptibility map

The susceptibility index map thus generated is validated by overlying the landslide inventory. The area under the ROC curve was calculated to be 0.727 (Fig. 8a), suggesting the landslide susceptibility model has a good level of accuracy in predicting the occurrence of landslides in the area. The susceptibility map is further validated using the landslide density distribution in different susceptibility classes (Fig. 8b). The distribution of maximum landslide density in the very high susceptibility class and conversely the lowest density in very low classes distinctly reflects the ability to predict landslide using the model.

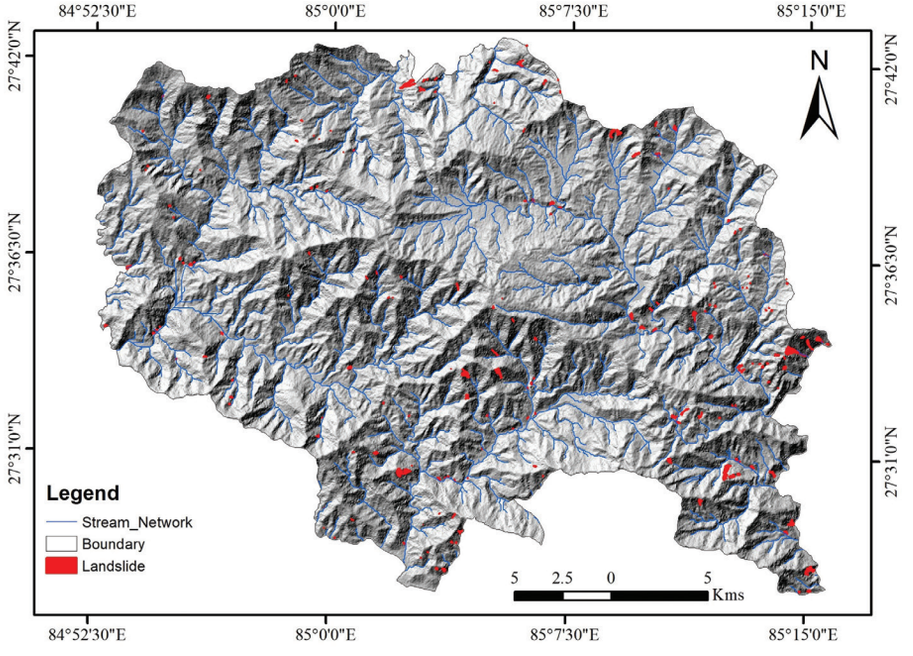

Fig. 6: Distribution of the landslide within the study area.

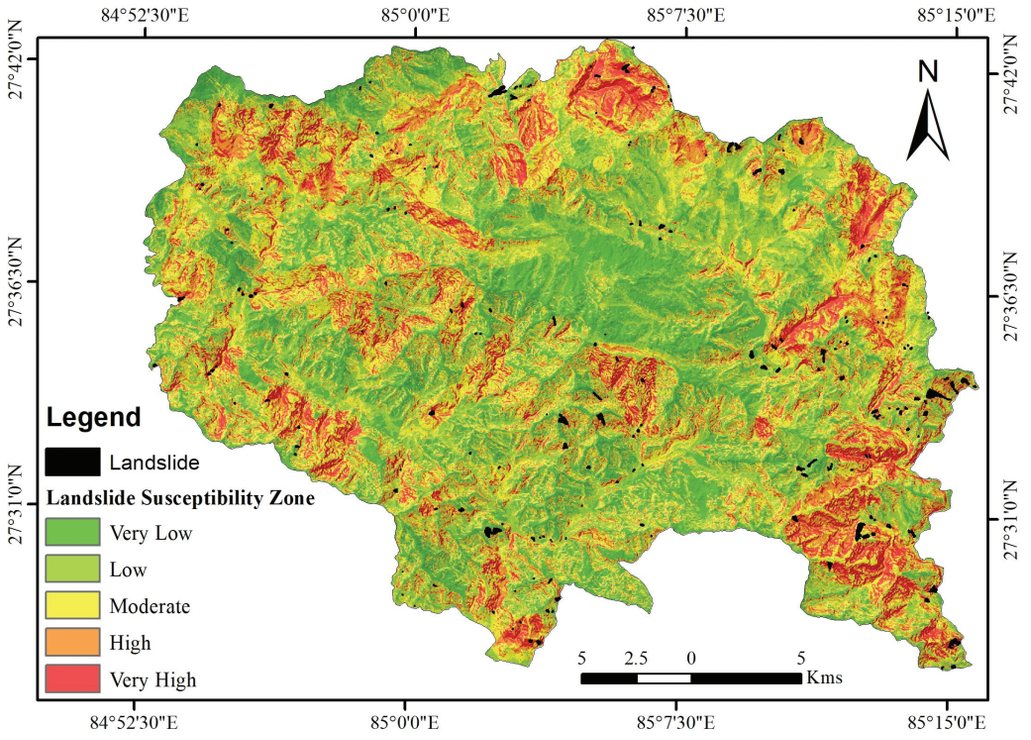

Fig. 7: Landslide susceptibility map prepared from the integration of different thematic layers under consideration.

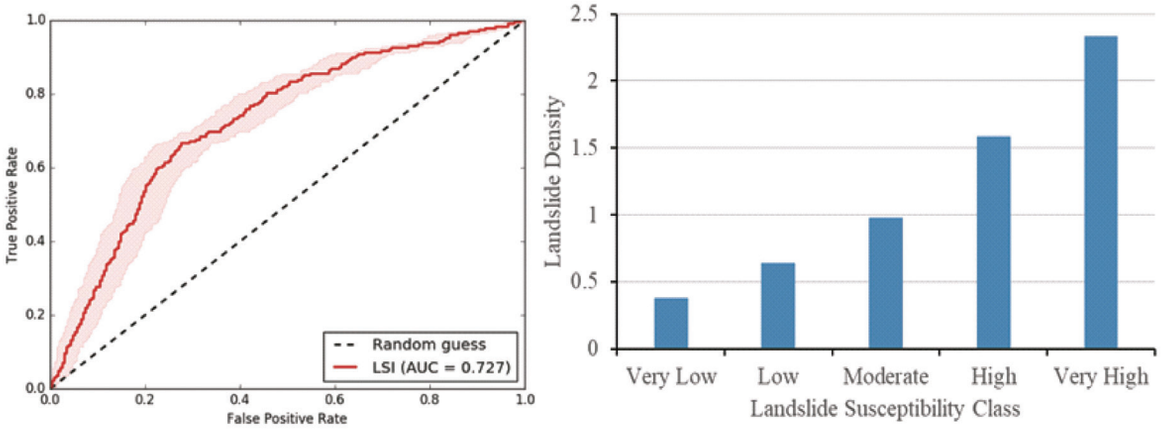

Fig. 8: Validation of the Landslide Susceptibility Map using a) Area under the ROC curve b) Distribution of landslide density in different susceptibility classes.

DISCUSSION

The landslide susceptibility analysis reveals that slopes within the 35°-45° class exhibit the highest percentage (33.5%) landslide, while the 0°-15° class has the lowest occurrence at 5.32%. This suggests that slopes between 35° and 45° are particularly vulnerable to landslides. The attribution of weights to each slope class is based on the understanding that landslide susceptibility increases with steeper slopes, aligning with the findings of Kanwal et al. (2016). Furthermore, the lowest landslide occurrence in the gentle slope surface can be attributed to reduced angle of repose that minimizes the shear stress in the soil making it more stable (Regmi et al., 2014). Analysis of slope aspects indicates that Southeast, South, East and Southwest facing slopes are most prone to landslides. This pattern is particularly relevant in the Himalayan region experiencing monsoon storms that enters from east and gradually move towards the west, which causes significant amount of precipitation on the south facing slopes, making the area more prone to landslide (Kayastha, 2012; Cook and David, 2013). The distribution of landslides is significantly influenced by land cover, with forested areas

typically experiencing maximum landslides compared to the other region. This could be attributed to the condition such as partial deforestation, unplanned road construction within the forested area compromising slope stability issues that has caused the landslide (Karsli et al. 2009; Meneses et al. 2019; Pacheco Quevedo et al., 2023). The occurrences of landslide are somehow evenly distributed within the convex and concave slopes and similar pattern has been identified in different studies (Nakileza and Nedala, 2020). This may be due to the water saturation at the slope base during intense rainfall increasing the chance of potential landslide and debris flow activities in the concave slope with soil or unconsolidated material. Meanwhile, the landslide distribution in convex slope may be attributed to the debris slide and rock slides along the steep slopes (Regmi et al., 2014). Analysis of the Topographic Position Index indicates that the landslide density is maximum along the river valley followed by the Hilltop/Spur. This distribution pattern is due to the occurrences of landslides within the river valley. Further the distribution of higher density in the hilltop or the spur could be linked with the seismic induced landslide, where the ground shaking is amplified along the ridgeline (Kritikos et al., 2015). Distribution of landslide density within different lithological units indicates higher densities within the rocks of the siwaliks followed by marble and dolomites of the Lesser Himalaya. This pattern can be well justified by the fragile nature of the rocks of siwaliks (Bhandari and Dhakal, 2018) and the highly fractured and jointed nature of the dolomite and marbles within the study area. Similarly, very low landslide density has been observed along the basic rocks (amphibolite and metagabbro) which correlates well with the high resistance to weathering and erosion.

CONCLUSIONS

Landslides represent a prevalent and significant natural hazard in mountainous regions like Nepal, often causing sudden and extensive damage. Within the study area, a total of 230 landslides, varying in size, were identified, covering approximately 1.62 square kilometers, equivalent to 0.2196% of the study area. About 18% area lies in very low susceptible zone followed by 29% in low, 26 % in moderate, 19% in high and 8% in very high susceptible zone. The model is well validated with 72% accuracy using area under the ROC curve.

The study concludes that the slope >35^{o}, southward facing slope, river valley, ridges and spurs are the most important landslide conditioning factor classes. Mostly high susceptible zones are distributed towards the eastern and southern part of the study area in comparison to other. The study recommends utilization of the landslide susceptibility maps for risk sensitive landuse planning (RSLUP) and landslide risk reduction efforts.

REFERENCES

Acharya, S. and Pathak, D., 2017, Landslide hazard assessment around MCT zone in Marsyangdi Riverbasin, west Nepal. Journal of Nepal Geological Society, v. 53, pp. 93-98. DOI: 10.3126/jngs.v53i0.23821

Acharya, T.D., Yang, I.T. and Lee, D.H., 2017, GIS-based landslide susceptibility mapping of Bhotang, Nepal using frequency ratio and statistical index method. Journal of the Korean Society of Surveying, Geodesy, Photogrammetry and Cartography, v. 35(5), pp. 357-364. https://doi.org/10.7848/ksgpc.2017.35.5.357

Akgun, A., Dag, S. and Bulut. F., 2010, Landslide susceptibility mapping for Ayvalik (Western Turkey) and its vicinity by multi-criteria decision analysis. Environmental Earth Sciences, v. 54, pp. 595–611. https://doi.org/10.1007/s12665-009-0373-1

Ayalew, L., Yamagishi, H., Marui, H. and Kanno. T., 2005, Landslides in Sado Island of Japan: Part II. GIS-based susceptibility mapping with comparisons of results from two methods and verifications. Engineering Geology, v. 81, pp. 432–445. https://doi.org/10.1016/j.enggeo.2005.08.004

Bhandari, P. B. and Dhakal, S., 2018, Lithological Control on Landslide in the Babai Khola Watershed, Siwaliks Zone of Nepal. American Journal of Earth Sciences, v. 5, pp. 54-64.

Bhandary, N.P., Yatabe, R., Hasegawa, S., Inagaki, H. and Shrestha, H.K., 2006, Characterization of Landslides and Roadside Slope Failures along the Highways in Central Nepal. In Proceedings of International Symposium on Geo-disasters: Infrastructure Management and Protection of World Heritage Sites, pp. 25-26.

Carson, M. and Kirkby, M., 1972, Hillslope Form and Process. Cambridge University Press, London.

Cook, N. and David B., 2013, The Atta Abad Landslide and Everyday Mobility in Gojal, Northern Pakistan. Mountain Research and Development, v. 33(4), pp. 372-380. https://doi.org/10.1659/MRD-JOURNAL-D-13-00013.1

Dahal, B. K. and Dahal, R. K., 2017, Landslide hazard map: tool for optimization of low-cost mitigation. Geoenvironmental Disasters, v. 4:8. doi: 10.1186/s40677-017-0071-3.

Das, S., Sarkar, S. and Kanungo, D.P., 2023, A critical review on landslide susceptibility zonation: recent trends, techniques, and practices in Indian Himalaya. Nat Hazards, v. 115, pp. 23–72 https://doi.org/10.1007/s11069-022-05554-x

García-Rodríguez M.J., Malpica J.A., Benito B. and Diaz M., 2008, Susceptibility assessment of earthquake-triggered landslides in El Salvador using logistic regression. Geomorphology, v. 95(3-4), pp. 172-191.

Glade, T. and Crozier, M. J., 2005, The nature of landslide hazard impact. Landslide hazard and risk, pp. 41-74.

Hong, H., Pourghasemi, H.R. and Pourtaghi, Z.S., 2016, Landslide susceptibility assessment in Lianhua County (China): a comparison between a random forest data mining technique and bivariate and multivariate statistical models. Geomorphology, v. 259, pp. 105–118. https://doi.org/10.1016/j.geomorph.2016.02.01.

Huang, F., Tao, S., Li, D., Lian, Z., Catani, F., Huang, J. and Zhang, C., 2022, Landslide susceptibility prediction considering neighborhood characteristics of landslide spatial datasets and hydrological slope units using remote sensing and GIS technologies. Remote Sensing, v. 14(18), 4436.

Kanwal S., Atif S. and Shafiq M., 2016, GIS based landslide susceptibility mapping of northern areas of Pakistan, a case study of Shigar and Shyok Basins. Geomatics, Natural Hazards and Risk, v. 8(2), pp. 348-366. doi: 10.1080/19475705.2016.1220023

Karsli, F., Atasoy, M., Yalcin, A., Reis, S., Demir, O. and Gokceoglu, C., 2009, Effects of land-use changes on landslides in a landslide-prone area (Ardesen, Rize, NE Turkey). Environmental Monitoring and Assessment, v. 156, pp. 241–255. https:// doi. org/ 10. 1007/s10661-008-0481-5

Kayastha, P., 2012, Application of fuzzy logic approach for landslide

susceptibility mapping in Garuwa sub-basin, East Nepal. Front. Earth Sci., v. 6, pp. 420–432. https://doi.org/10.1007/s11707-012-0337-8

Kayastha, P., Dhital, M.R. and De Smedt, F., 2012, Landslide susceptibility mapping using the weight of evidence method in the Tinau watershed, Nepal. Nat Hazards, v. 63(2), pp. 479– 498. https://doi.org/10.1007/s11069-012-0163-z

KC. M., Silwal, C.B., Dangi, P. and Pathak, D., 2024, Comparing Frequency Ratio and Analytical Hierarchy Models for Landslide Susceptibility in the Dharan Sub-Metropolitan Region of Eastern Nepal. Journal of Development Innovations, v. 8(1), pp. 1-17. http://doi.org/10.69727/jdi.v8i1.103

Komac, M., 2006, A landslide susceptibility model using the analytical hierarchy process method and multivariate statistics in perialpine Slovenia. Geomorphology, v. 74, pp. 17–28. https://doi.org/10.1016/j.geomorph.2005.07.005

Kritikos, T., Robinson, T.R. and Davies, T.R.H., 2015, Regional coseismic landslide hazard assessment without historical landslide inventories: A new approach. J. Geophys. Res. Earth Surf., v. 120, pp. 711–729. https://doi.org/10.1002/2014JF003224

Lawal, M.A., Oshomoji, A.O., Akinlalu, A.A., Omosanya, K.O., Ndukwe, O.S., Adiat, K.A.N. and Mosuro, G.O., 2022, A simplified GIS and google-earth-based approach for lineaments and terrain attributes mapping in a basement complex terrain. Scientific Reports, v. 12(1):15801. https://doi.org/10.1038/s41598-022-20057-2

McAdoo, B. G., Quak, M., Gnyawali, K. R., Adhikari, B. R., Devkota, S., Rajbhandari, P. L. and Sudmeier-Rieux, K., 2018, Roads and landslides in Nepal: how development affects environmental risk. Nat. Hazards Earth Syst. Sci., v. 18, pp. 3203–3210. https://doi.org/10.5194/nhess-18-3203-2018.

Meneses, B.M., Pereira, S. and Reis, E., 2019, Effects of different land use and land cover data on the landslide susceptibility zonation of road networks. Nat Hazards Earth Syst Sci., v. 19, pp. 471–487. https:// doi. org/10.5194/nhess-19-471-2019

Muñoz-Torrero Manchado, A., Allen, S., Ballesteros-Cánovas, J.A., Dhakal, A., Dhital, M.R. and Stoffel, M., 2021, Three decades of landslide activity in western Nepal: new insights into trends and climate drivers. Landslides, v. 18, pp. 2001–2015. https://doi.org/10.1007/s10346-021-01632-6

Nakileza, B.R. and Nedala, S., 2020, Topographic influence on landslides characteristics and implication for risk management in upper Manafwa catchment, Mt Elgon Uganda. Geoenviron Disasters, v. 7:27. https://doi.org/10.1186/s40677-020-00160-0

Neaupane, K.M. and M. Piantanakulchai., 2006, Analytic network process model for landslide hazard zonation. Engineering Geology, v. 85, pp. 281–294. https://doi.org/10.1016/j.enggeo.2006.02.003

Pacheco Quevedo, R., Velastegui-Montoya, A., Montalván-Burbano, N., Morante-Carballo, F., Korup, O. and Daleles Renno, C., 2023, Land use and land cover as a conditioning factor in landslide susceptibility: a literature review. Landslides, v. 20, pp. 967–982. https://doi.org/10.1007/s10346-022-02020-4

Pathak, D., 2016, Knowledge based landslide susceptibility mapping in the Himalayas. Geoenviron Disasters, v. 3:8. https://doi.org/10.1186/s40677-016-0042-0

Pourghasemi, H.R., Moradi, H.R. and Fatemi Aghda, S.M., 2013, Landslide susceptibility mapping by binary logistic regression, analytical hierarchy process, and statistical index models and assessment of their performances. Natural Hazards, v. 69(1), pp. 749-779. https://doi.org/10.1007/s11069-013-0728-5

Pourghasemi, H.R., Pradhan, B., Gokceoglu, C. and Deylami Moezzi, K., 2012, Landslide susceptibility mapping using a spatial multi criteria evaluation model at Haraz Watershed, Iran. Terrigenous Mass Movements. Springer, Berlin, Heidelberg, pp. 23–49. https://doi.org/10.1007/978-3-642-25495-6_2

Pradhan, A.M.S. and Kim, Y.-T., 2020, Rainfall-Induced Shallow Landslide Susceptibility Mapping at Two Adjacent Catchments Using Advanced Machine Learning Algorithms. ISPRS Int. J. Geo-Inf., v. 9:569. https://doi.org/10.3390/ijgi9100569

Pradhan, A.M.S., Dawadi, A. and Kim, Y.T., 2012, Use of different bivariate statistical landslide susceptibility methods: A case study of Kulekhani watershed, Nepal. Journal of Nepal Geological Society, v. 44, pp. 1-12.

Regmi, A.D. and Poudel, K., 2016, Assessment of landslide susceptibility using GIS-based evidential belief function in Patu Khola watershed, Dang, Nepal. Environmental Earth Sciences, v. 75, pp. 1-20. https://doi.org/10.1007/s12665-016-5562-0

Regmi, A.D., Devkota, K.C., Yoshida, K., Pradhan, B., Pourghasemi, H.R., Kumamoto, T. and Akung, A., 2014, Application of frequency ratio, statistical index, and weights-of-evidence models and their comparison in landslide susceptibility mapping in Central Nepal Himalaya. Arab J Geosci., v. 7, pp. 725–742. https://doi.org/10.1007/s12517-012-0807-z

Regmi, A.D., Yoshida, K., Pourghasemi, H.R., Dhital, M.R. and Pradhan, B., 2014, Landslide susceptibility mapping along the Bhalubang—Shiwapur area of mid-Western Nepal using frequency ratio and conditional probability models. Journal of Mountain Science, v. 11, pp. 1266-1285. https://doi.org/10.1007/s11629-013-2847-6

Regmi, N.R., Giardino, J.R., McDonald, E.V. and Vitek, J.D., 2014, A comparison of logistic regression-based models of susceptibility to landslides in western Colorado, USA. Landslides, v. 11, pp. 247–262. https://doi.org/10.1007/s10346-012-0380-2

Roback, K., Clark, M.K., West, A.J., Zekkos, D., Li, G., Gallen, S.F. and Godt, J.W., 2018, The size, distribution, and mobility of landslides caused by the 2015 Mw7. 8 Gorkha earthquake, Nepal. Geomorphology, v. 301, pp. 121-138. https://doi.org/10.1016/j.geomorph.2017.01.030

Roy, D., Sarkar, A., Kundu, P., Paul, S. and Sarkar, B.C., 2023, An ensemble of evidence belief function (EBF) with frequency ratio (FR) using geospatial data for landslide prediction in Darjeeling Himalayan region of India. Quaternary Science Advances, v. 11: 100092. https://doi.org/10.1016/j.qsa.2023.100092

Saaty, T. L., 1977, A scaling method for priorities in hierarchical structures. Journal of Mathematical Psychology, v. 15(3), pp. 234–281. https://doi.org/10.1016/0022-2496(77)90033-5

Saaty, T. L., 1980, The Analytic Hierarchy Process: Planning, Priority Setting, Resource Allocation. McGraw-Hill International Book Co., New York, London.

Saaty, T. L., 2000, Fundamentals of Decision Making und Priority Theory with the Analytic Hierarchy Process , v. vi , University of Pittsburgh .

Seif, A., 2014, Using Topography Position Index for Landform Classification (Case study: Grain Mountain). Bull. Env. Pharmacol. Life Sci., v. 3, pp. 33-39.

Shrestha, N., Bhatta, U.D., Ghimire, B.N.S. and Karna, A.K., 2024,

Dam Break Flood Hazard Mapping and Vulnerability Analysis in Kulekhani Dam, Nepal. In: Nagabhatla, N., Mehta, Y., Yadav, B.K., Behl, A., and Kumari, M. (eds) Recent Developments in Water Resources and Transportation Engineering. TRACE 2022. Lecture Notes in Civil Engineering, Springer, Singapore, v. 353, pp. 81-95. https://doi.org/10.1007/978-981-99-2905-4_7

Silwal, C.B., Nepal, M., Pathak, D., Karkee, B., Dahal, K. and Acharya, S., 2023, Groundwater potential zonation in the Siwalik of the Kankai River Basin, Eastern Nepal. Water Supply, v. 23 (6), pp. 2332–2348. doi: https://doi.org/10.2166/ws.2023.137

Sthapit, K. M., 1996, Sedimentation monitoring of Kulekhani reservoir. In International Conference on Reservoir Sedimentation, Fort Collins, Colorado, USA

Stöcklin, J. and Bhattarai, K.D., 1980, Geology of Kathmandu area and central Mahabharat Range, Nepal Himalaya. HMG Nepal/ UNDP report, 64p.

Thapa, S., Karna, A.K. and Dahal, B.K., 2022, Evaluation of Different Landslide Susceptibility Analysis Methods: A Case Study of Bagmati Rural Municipality. Journal of Engineering Technology and Planning, v. 3(1), pp. 44-59.

Vaidya, R.A., Shrestha, M.S., Nasab, N., Gurung, D.R., Kozo, N., Pradhan, N.S. and Wasson, R.J., 2019, Disaster risk reduction and building resilience in the Hindu Kush Himalaya. The Hindu Kush Himalaya assessment: Mountains, climate change, sustainability and people, pp. 389-419. https://doi.org/10.1007/978-3-319-92288-1_11

Yesilnacar, E. and Topal, T., 2005, Landslide Susceptibility Mapping: A Comparison of Logistic Regression and Neural Networks Methods in a Medium Scale Study, Hendek Region (Turkey). Engineering Geology, v. 79(3-4), pp. 251-266. https://doi.org/10.1016/j.enggeo.2005.02.002